Simulation Silicon Surfactant Rule on Polyurethane Foaming Reactions

Al-Moameri, Harith H.*•; Zhao, Yusheng ; Ghoreishi, Rima;
Suppers, Galen J. Suppes
Department of Chemical Engineering, University of Missouri-Columbia, W2033 Lafferre Hall, Missouri 65211, COLUMBIA

ABSTRACT: *During the foaming process of polyurethane, the surfactant plays a significant role in stabilizing and setting the foam. Simulation this role helps in better predicting the final performance and optimum foam formulation. The relation between the amount of surfactant added to the formulation and the surface tension was studied experimentally by using the capillary rise method to develop a simulation model. This model was aimed to study the critical role of the mechanism that surfactants have in the initial stages of gel formation and through the point where viscosity is high enough to create resistance to support the foams. Bubble sizes were calculated based on the number of nucleation sites, gas generation rate, surface tension, and inner bubble pressure. Since important properties of polyurethane foam, such as compressive strength, closed-cell content, and thermal conductivity can be related to the bubble sizes, this model can be used to predict foam performance and to develop new foam formulations.*

KEYWORDS: *Surfactant; Polyurethane; Foam; Collapse; Collision.*

INTRODUCTION

The polyurethane foaming process involves two competing reactions (gel reaction and blow reaction) [1]. The gel reaction of polyurethane involves the reaction of an isocyanate moiety with an alcohol moiety to form a urethane linkage [2-5]. In the foaming reaction, the isocyanate moiety reacts with one molecule of water to yield a thermally unstable carbamic acid which decomposes to give amine functionality, carbon dioxide, and heat [6-10]. The carbon dioxide gas expands the nucleation sites to form a foam. The bubbles occupy over 95% of the final volume of the foam product [11-13]. The four stages of foaming are:

(1) Bubble generation and growth,

(2) Packing of the bubble network and cell window stabilization,

(3) Polymer stiffening and cell opening,

(4) Final curing [14].

Fig. 1 provides a schematic diagram of the four stages of the foaming process[15-17]. In rigid foams, most of the cells or bubbles are not broken; they resemble inflated balloons or soccer balls, piled together in a compact configuration. Both the closed cells and the solid resin walls contribute to the ultimate strength of the rigid foam.

In polyurethane foaming systems, the common surfactants are the silicone surfactants (consists of polydimethylsiloxane (PDMS) backbone) and the polyethylene oxide-co-propylene oxide random copolymer grafts [18]. The typical structures of the silicone surfactants are shown in Fig. 2. The surfactants have

***** *To whom correspondence should be addressed.*
+ E-mail: hha46d@mail.missouri.edu ; almoamerih@gmail.com
● *Other Address: Materials Engineering Department, College of Engineering, Mostansiriyah University, Baghdad, IRAQ*
1021-9986/2021/4/1256-1268 13/$/6.03

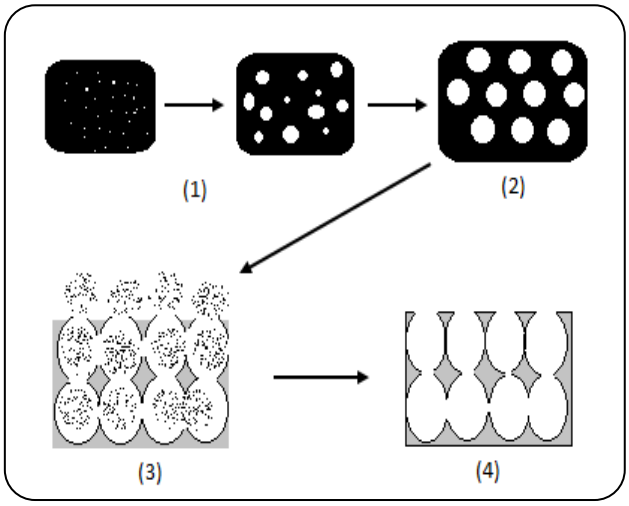

Fig. 1: Schematic diagram of the four stages of foam foaming.

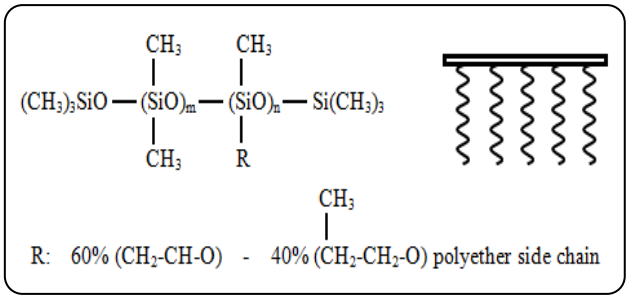

Fig. 2: Typical structure of silicone surfactant used in polyurethane foaming.

no impact on the reaction kinetics of polyurethane foaming reaction [19]; however, foams are often experienced catastrophic coalescence and foam collapse in the absence of these surfactants.

These surfactants concentrate at the air-resin interface and assist with both bubble generation and bubble/cell stabilization in the polyurethane foam-forming process. The structure of the silicone surfactant impacts the final mechanical properties of the foam, such as air permeability and foam cell size [11]. The higher silicon content of surfactants provides lower surface tension which increases the number of air bubbles introduced during mixing. Entrain gases (e.g. nitrogen) in the resin phase serves as the starting point for foam cell growth. As a result, the cured polyurethane foam made with higher silicon content surfactant has a smaller bubble size. Besides, silicone surfactant reduces the cell "window" drainage rate due to the surface tension gradient along with the cell window.

The primary role of silicone surfactants in rigid formulations are cell size control (providing a fine-celled structure with a narrow cell size distribution) and emulsification. A significant amount of gravitational and surface energy is adsorbed during foam formation. In polyurethane foams, this energy is provided by high shear mixing and the release of chemical energy during the formation of the polyurethane.

The earliest interfacial process is the initial formation of bubbles in the liquid. Kanner and coworkers demonstrated that there is no spontaneous nucleation of the bubbles in polyurethane foams; the bubbles have to be stirred in [20,21]. These initial bubbles are small, their diameters being on the micrometer scale. Once bubbles have formed, they must remain stable during their growth phase. As CO_2 gas is formed in the blowing reaction, it expands these tiny bubbles. They can also expand when auxiliary blowing agents such as pentane volatilize. The expansion of the bubbles increases the overall surface area; the total surface energy absorbed can be lessened by reducing the energy per unit area of the liquid (or equivalently, the surface tension). In polyurethane foams, the surface tension of the liquid is reduced by the addition of silicone surfactants. Fig. 3 shows the surface tension isotherm, which is the dependence of σ on lnC [22,23], where σ is the surface tension of the solution, and C is the concentration of surfactant. The surface tension of the solution decreases with the crease of the concentration of surfactant molecules in the system. The concentration at which the formation of the micelles starts is called Critical Micelle Concentration (CMC). For C lower than the CMC, surfactants are distributed between the bulk of the solution and the surface. After C reaches CMC, all added "excess" surfactants form micelles so that the bulk concentration of the individual surfactant molecules is constant and equal to the CMC. The surface concentration also reaches the saturation level.

As the surface tension decreases, the number of the generated bubbles per unit volume of solution increases. The energy required to generate the bubble surface with radius r is $4\pi r^2\sigma$. Surfactants with higher silicone/polyether ratios will give a lower surface tension value and thus reduce bubble generation energy. As a result, a higher bubble count was obtained after mixing for systems with lower surface tension. For a molded foam, at a fixed energy input, reduction of the surface tension of

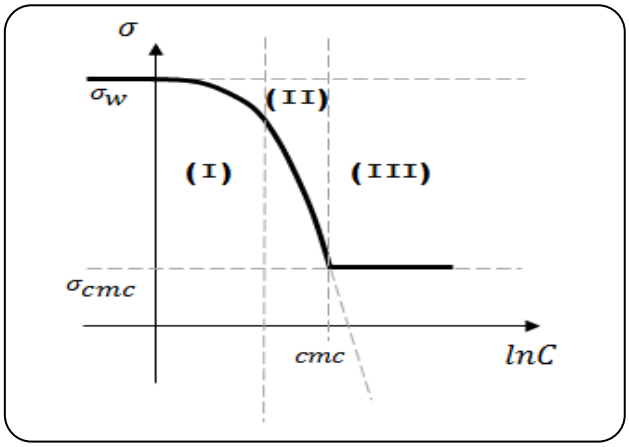

Fig. 3: Schematic representation of typical surface tension isotherm.

the liquid results in the formation of more and necessarily smaller bubbles as the available surface area is increased. For a free-rise foam, a reduction in surface tension can result in an increase in foam volume and/or a decrease in bubble size. It has been shown that the addition of a silicone surfactant to a polyether polyol allows five to seven times more gas to be mixed with the polyol than when the surfactant is absent. This increase in foam volume is consistent with the reduction of liquid surface tension by the surfactant. The stability of foam is inversely proportional to the rate at which surface and gravitational energy are released. Any process that reduces the surface area of a foam releases energy. These processes include bubble coalescence and the diffusion of gas from smaller to more giant bubbles. Gravitational energy is released during the drainage of liquid down the foam.

For a surfactant to aid in the growth and stabilization of polyurethane foam, it must reduce the surface tension of the foaming liquid, which is predominantly a polyether polyol. The surface tension of these polyols ranges from 33 to 40 mN/m. This value is so low that the adsorption of hydrocarbon-based surfactants cannot further reduce it. Essentially, they are not surface-active in this medium. However, silicone surfactants can reduce the polyol surface tension to a much lower value of 21-25 mN/m [23,24]. A requirement for these surfactants, allowing them to stabilize the foam is to reduce the surface tension of the liquid polyether polyols by 8-12 mN/m. The adsorption of these surfactants at the polyol-air interface appears to yield a molecular configuration of the surfactant where the siloxane portion is folded over itself. This adsorption also increases the surface viscoelasticity, which aids in stabilizing the foam. These surfactants also appear to be active at the water-polyol and urea-polyol interfaces. This activity increases the miscibility of water in the polyol and prevents a catastrophic collapse of the foam after the onset of urea phase separation.

THEORETICAL SECTION

Methodology

The capillary rise method is used to measure the surface tension of sample solutions. The adhesive force draws water up the sides of the glass tube to form a meniscus. The cohesive force tries to minimize the distance between the water molecules by pulling the bottom of the meniscus up against the force of gravity. The following relationship describes the upward forces of the surface tension:

$$F_{up} = \sigma (2\pi r) \cos\theta \quad (1)$$

Where σ is the liquid-air surface tension at 20°C2πr is the circumference of the tube, and θ is the contact angle of water on glass. The opposing force down is given by the force of gravity on the water that is pulled above the reservoir level.

$$F_{down} = \rho g \left(h \pi r^2 \right) \quad (2)$$

In Eq. (2), ρ = 1000 kg/m^3 is the density of water, g= 9.8 m/s^2 is the acceleration due to gravity, and ($h\pi r^2$) is the volume of the water in the column above the reservoir.

To measure the surface tension of a liquid, the height of the liquid rises in a capillary tube is measured. By setting the two forces above equal (Eq. (1) and Eq. (2)), surface tension can be calculated. For pure water and clean glass, the contact angle is nearly zero. In a typical lab, this may not be the case, but θ is small, and we assume that cosθ is close to 1.

$$\sigma = \frac{\rho g r}{2} \frac{h}{\cos\theta} \approx \frac{\rho g r}{2} h \quad (3)$$

Water/surfactant and polyol/surfactant solutions with different surfactant loadings were prepared, and the surface tension of these solutions was measured using the capillary rise method. A figure of surface tension versus ln(Csurf) was plotted to evaluate the relationship between surface tension and surfactant concentration. Capillary tubes (O.D.=1.00mm, I.D.=0.50mm, L=7.5cm) were used in the experiment.

Table 1: Foaming formulation of rigid polyurethane foam

B-side Materials	Weight/g
Polyol (Mwt:360, Fn:4.5)	35
Dimethylcyclohexylamine (Cat8 gelling catalyst)	0.12
Pentamethyldiethylenetriamine (Cat5 blowing catalyst)	0.32
Surfactant	0.1, 0.2, 0.4, 0.6
Fire Retardant	2
Distilled Water (Blowing Agent)	1.6
A-side Material	
Standard Polymeric MDI (MW:364.5, Fn:2.7)	59.8

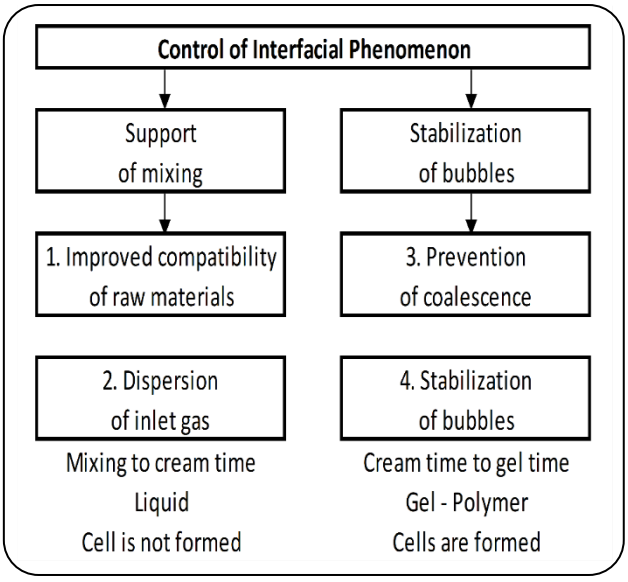

Fig.4: Four roles of surfactant in the urethane foaming process.

Foam samples with different amounts of surfactant were prepared to evaluate the relationship between surface tension and cell size. Foam samples with different mixing times (5, 10, 15, 25 seconds) were also prepared and evaluated. The foam recipe was listed in Table 1.

Modeling

Surfactants are known to be important in urethane formulations. Fig. 4 shows four roles of surfactants in the urethane foaming process:

- Emulsification – improving the compatibility of raw materials
- Nucleation of bubbles
- Prevention of coalescence (slow-down of diffusion)
- Stabilization

This modeling focuses on three key aspects:

- Surfactants are impacting the number of nucleation sites and bubble radius for cell growth.
- Surfactants are impacting the stability of bubbles and the tendency for bubbles to coalesce.
- Surfactants are impacting the escape of bubbles by rising to the surface of the forming foam.

Bubble growth

Based on the previous research results mentioned above, several assumptions were made in the modeling calculations: (1) Bubbles are introduced by the process of mixing the foam components and are sufficient to account for all of the cells in the final foam. (2) Nucleation of bubbles is essentially absent and is thermodynamically unfavorable under the conditions of foam formation. New bubbles are not seen during the formation of foam. It is simpler for carbon dioxide gas to diffuse from solution to existing bubbles than to nucleate new bubbles. (3) When bubble introduction by mixing is deliberately held to a minimum, the rate of carbon dioxide evolution is decreased considerably, and the foam produced is grossly coarse celled.

According to the results of Kanner's study on average bubble size distribution [20], the initial bubble radius was found to be $3.4*10^{-3}$ cm and a cell count of $1.4*10^{8}$ in the solution with a surface tension of 25 dynes/cm after 10 seconds mixing at 1200 rpm. The energy absorbed by these generated bubbles were:

$$W = Nc \times 4 \times \pi \times r^2 \times \sigma =$$

$$1.4 \times 10^8 \times 4 \times \pi \times \left(3.4 \times 10^{-3}\right)^2 \times 0.025 = 0.05J$$

where W is the energy introduced by mixing which is directly proportional to mixing time at a constant stirring speed, Nc is the number of nucleation sites, r is the bubble radius, and σ is the surface tension of solutions. Assume that the same stirring condition was applied and therefore, the same energy was introduced. Then the number of nucleation sites will be dependent on the surface tension of solutions.

$$Nc = \frac{W}{4 \times \pi \times r^2 \times \sigma} \quad (4)$$

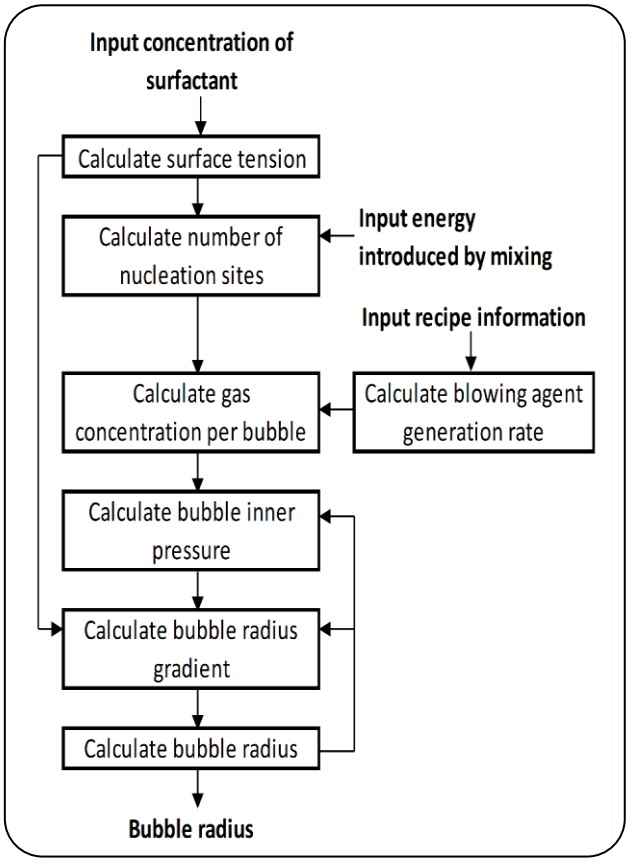

Fig. 5: Algorithm for calculating bubble radius during the foaming process

During the bubble growth process, a force balance can be written at the bubble surface [25]:

$$p_b - p_a + \tau_{rr} = \frac{2\sigma}{r} \quad (5)$$

in which p_b is the pressure in the bubble, p_a is the pressure of the liquid at the bubble surface, and τ_{rr} is the radius component of the viscous stress tensor in the liquid. The radius component of the stress tensor within the bubble was neglected since we take the gas viscosity to be zero. And in a Newtonian liquid

$$p_\infty - p_a = -4\mu \times \frac{1}{r} \times \frac{dr}{dt} \quad (6)$$

where p_∞ is the ambient pressure and μ is the Newtonian viscosity. Substitution of Equation 5 into Equation 6 results in an expression:

$$p_b - p_\infty - \frac{2\sigma}{r} = 4\mu \times \frac{1}{r} \times \frac{dr}{dt} \quad (7)$$

Based on the ideal gas law, inner bubble pressure can also be obtained. Equation 7 was calculated in the MATLAB program in addition to the temperature and foam height profiles [26-28]. Fig. 5 shows the algorithm for calculating the bubble radius during the foaming process.

Film thinning

The rate of thinning of films affects the stability and lifetimes of dispersions such as foams and emulsions. Reynolds, in his century-old investigation of the theory of lubrication, derived the following expression for the velocity of thinning of a plane-parallel, tangentially immobile fluid film [29].

$$V_{Re} = \frac{dh}{dt} = \frac{2h^3}{3\mu r^2}\Delta P \quad (8)$$

Where h is the film thickness, t is the time, μ is the dynamic viscosity, r is the radius of the film, and ΔP is the pressure drop causing the drainage. The pressure drop (ΔP driving force per unit area) consists of the capillary pressure, buoyancy (if present), and the disjoining pressure that owes its origin to the London van der Waals interactions and becomes significant only for very thin films (h <1000 $\dot{A}$). While numerous investigations regarding foam and emulsion films have employed Reynold's equation, recent experimental studies have all concluded that Equation 8 is essentially incorrect for describing the drainage from thin films, especially for films with radii greater than 10^{-2} cm. Therefore, *Ruckenstein* and *Sharma* [30] developed a revised overall film thinning equation (Equation 9).

$$V_t = V_{Re}\left[1 + 7.35\left(\frac{r}{\lambda}\right)\left(\frac{\epsilon_t}{h}\right)\right] \quad (9)$$

Where λ is the characteristic length (wavelength) of the thickness non-homogeneities, which was indirectly inferred to be about $5*10^{-3}$ cm, $\epsilon_t \approx 2\epsilon = (797r^{0.25} - 209)\dot{A}$ is the total amplitude (on both faces of the film) of the thickness non-homogeneities and is given as a function of the film radius by correlation.

Initial average film thickness can be calculated by Eq. (10) based on resin phase volume, initial bubble radius, and the number of nucleation. The actual film thickness are assumed to follow a normal distribution; the corresponding probability values (D_i) are listed in Table 2.

Table 2: Distribution of actual film thickness

h_{0i}	0.4	0.6	0.8	1.0	1.2	1.4	1.6
D_i	0.0062	0.0606	0.2417	0.3830	0.2417	0.0606	0.0062

$$h_{0,ave} = \frac{V_l}{4\pi r^2 \times N_c} \quad (10)$$

Redoev et al. [31] measured directly the velocity of thinning at the critical thickness, i.e., thickness at which the primary film ruptures due to the dispersion force-mediated growth of surface corrugations. Their data for the critical thickness are well represented by the following correlation ($10^{-2} < R < 10^{-1}$ cm),

$$\log h_c = 0.1145 \log R + 2.6598 \quad (11)$$

Where h_c is the critical thickness in angstroms and *R* is in centimeters. When a thinning film reaches the critical film thickness, it will be regarded as an open-cell, and therefore, closed-cell content can be calculated based on final film thickness. Fig. 6 presents the algorithm for calculating film thickness and closed cell content.

Bubble rising

The deformation and coalescence process is similar in a short distance in polyurethane foaming. Also, the rising velocity of the lower bubble is higher than the upper bubble, and the coalescence time of two bubbles with the same diameters increases as the center distance increases.

For two bubbles of different volumes within a certain distance in the resin phase, when the bigger bubble is located beneath a smaller bubble at the initial foaming time, the bigger bubble moves upward while the smaller bubble moves upward first and then moves downward before two bubbles coalescence. If the smaller bubble is located beneath, the bigger bubble at the initial foaming time, the two bubbles move upward with a higher velocity of the bigger bubble and bubble coalesce cannot happen.

The rise of a bubble in the liquid is a function of several parameters viz. bubble characteristic (size and shape), properties of gas-liquid systems (density, viscosity, surface tension, the concentration of solute, the density difference between gas and liquid), liquid motion (direction), and operating conditions (temperature, pressure, gravity) [32]. In surface tension force dominant range:

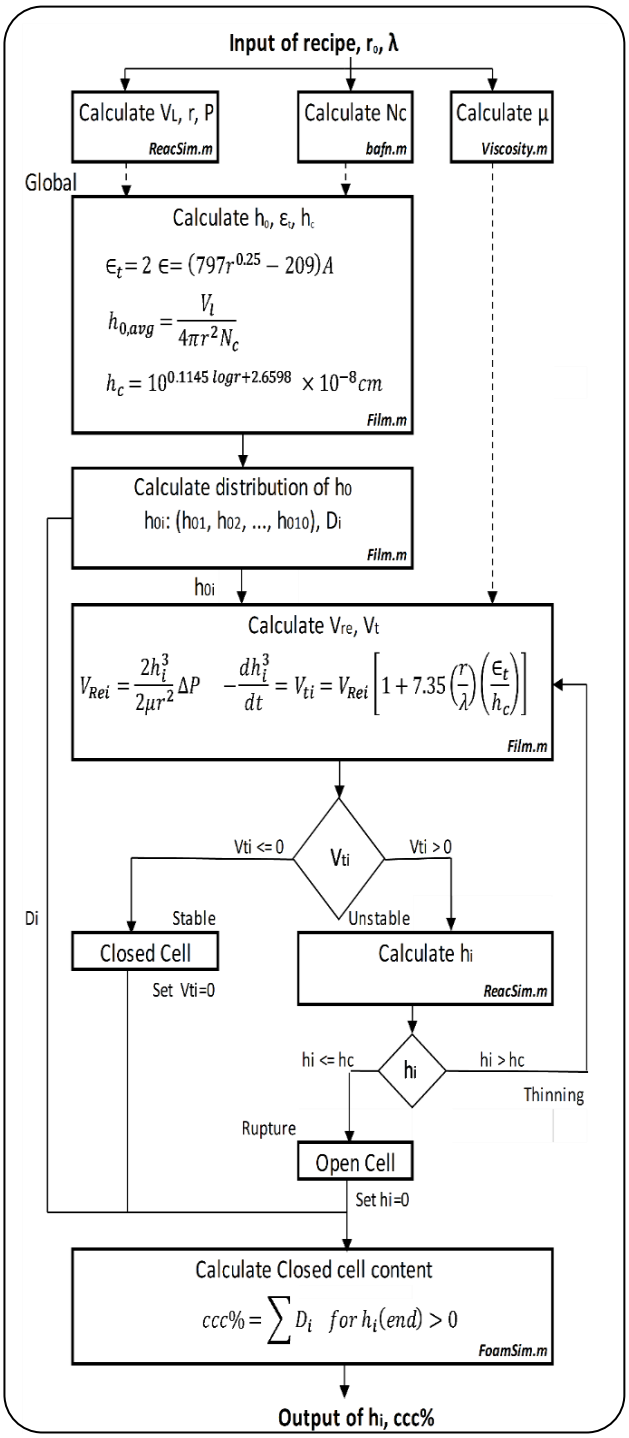

Fig. 6: Algorithm for calculating film thickness and closed cell content.

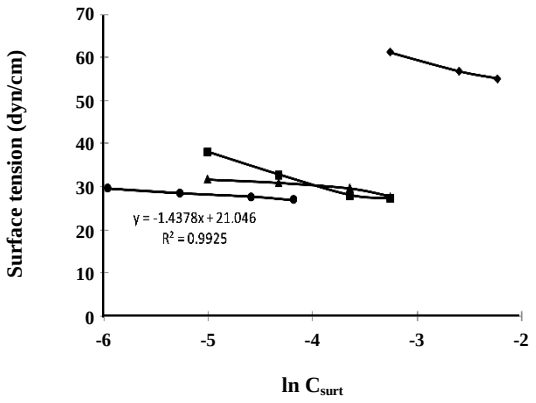

Fig. 7: Surface tension versus ln(Csurf) in different solutions. Symbols "♦■▲●" refer to experimental data for water, polyol 1, polyol 2, and mixture respectively.

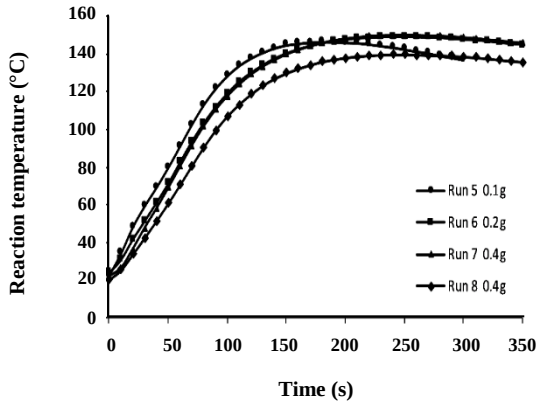

Fig. 8: Temperature profiles of foams with different concentration loadings.

Fig. 9: Longitudinal sections of foams with different surfactant loadings

$$V_r = \sqrt{\frac{2\sigma}{\rho_L d} + \frac{(\rho_L - \rho_G) g d}{2}} \quad (12)$$

In viscosity dominant range:

$$V_r = \frac{1}{18} \frac{g d^2 (\rho_L - \rho_G)}{\mu_L} \quad (13)$$

where g is the acceleration due to gravity, d is the diameter of the bubble, μ_L is the dynamic viscosity of the liquid, ρ_L is the density of liquid and ρ_G is the density of the gas.

RESULTS AND DISCUSSION

Experimental Data

Surface tension was plotted as a function of ln(C_{surf}) in Fig. 7. The surface tension of the solution decreased as the surfactant amount increasing. Within the range of surfactant amounts studied, the surface tension was a linear function of ln(C_{surf}), and therefore the surface tension can be calculated based on the concentration of surfactant in solutions as

$$\sigma = -1.4378 \times \ln C_{surf} + 21.046 \quad (14)$$

Fig. 8 presents the temperature profiles of the foams with different surfactant loadings. The results indicated surfactant had no significant impact on reaction kinetics and thermodynamics, which agreed with the assumption made in modeling calculation.

Fig. 9 shows the longitudinal sections of the foams with different surfactant loadings. Foam #5 had the lowest surfactant loading, thus leading to the least nucleation sites (number of bubbles). As the volume changes were the same, the bubbles in foam #5 had the largest radius. Differences between foams #6-#8 cannot be told easily by naked eyes, and therefore microscope observations were performed (Fig. 10). The bubble size of foam #5 was too

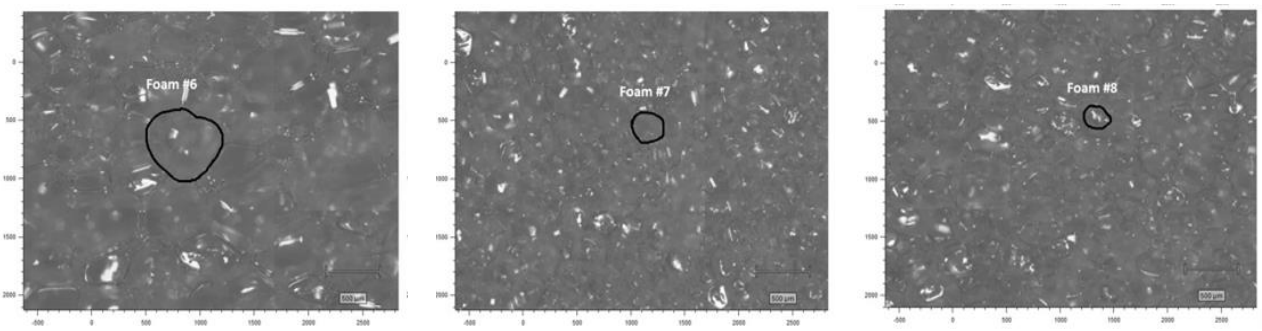

Fig. 10: Microscope observations of foams with different surfactant loadings.

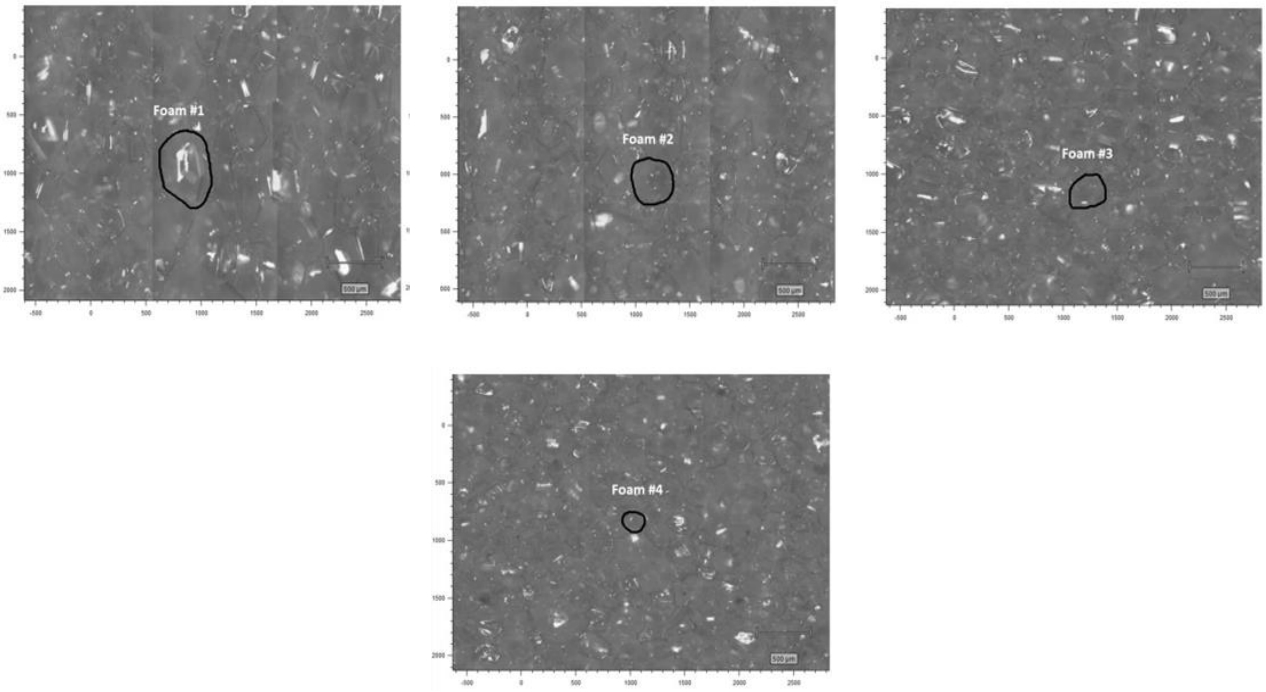

Fig. 11: Microscope observations of foams with a different mixing time.

big to take a microscope observation and therefore, was not presented.

Fig. 11 shows microscope observations of foams (#1-#4) which have different mixing times (5, 10, 15, 25 seconds) and the same control formulation (0.6 g surfactant). Longer mixing time introduced more nucleation cells and led to a smaller bubble radius as the volume changes were the same.

Preliminary Modeling Results

Simulation results from MATLAB program were presented in Fig. 12. The results included temperature, foam height, bubble radius, inner bubble pressure, and film thickness profiles. In the beginning, carbon dioxide was generated rapidly by blow reaction, and the gas volume change expanded the existing bubbles. At a later time stage, when viscosity was large enough to provide the strength bubbles stopped growth and foam stopped rising. After setting bubble radius stayed as a constant, and then inner bubble pressure slightly decreased as the temperature cooled down. Temperature and foam height results agreed with experimental data, and therefore bubble radius and pressure results were believed to be reasonable.

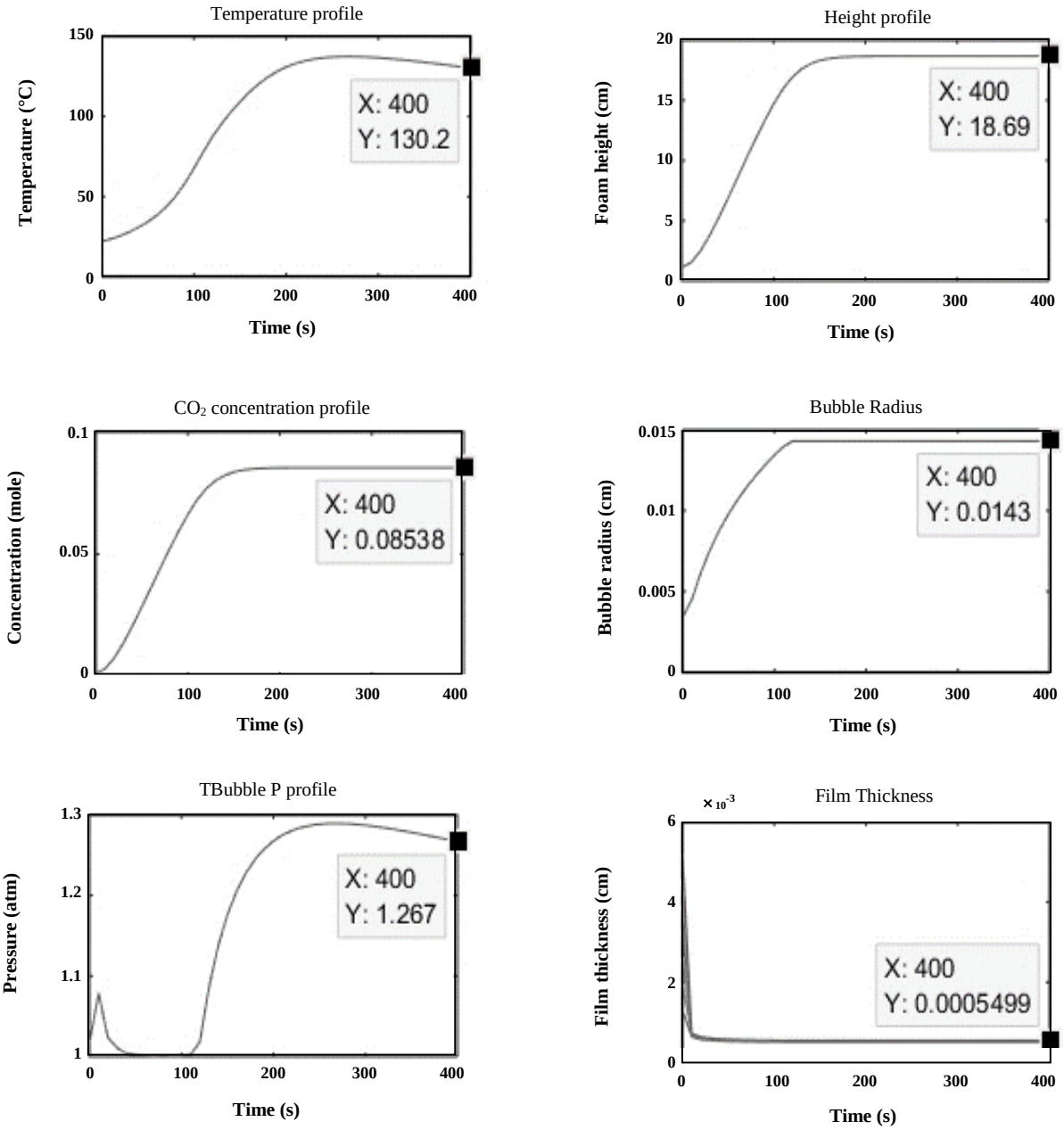

Fig. 12: Simulation results from MATLAB program.

Mixing time and surfactant amount were changed respectively to get the simulated bubble radius of foams #1-#8. Twenty bubbles were chosen from Fig. 10 and Fig. 11 to calculate the average experimental radius. Fig. 13 shows a comparison of experimental and modeling bubble radius as mixing time increases. Fig. 14 shows a comparison of experimental and modeling bubble radius as surfactant amount increasing.

The simulation successfully predicted the final bubble radius as long as the appropriate surfactant amount was used. Simulation of bubble growth is not sufficient to model the complicated foaming process, and therefore modes of failure need to be taken into consideration. Film thinning is considered as one possible source of bubble coalescence and rupture. However, based on the simulation results from Fig. 12, the final film thickness is about 55000$\dot{A}$,

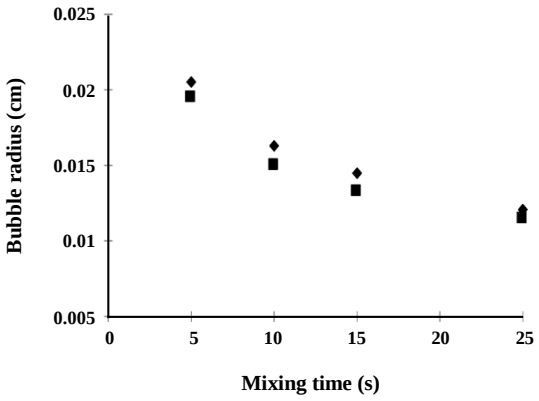

Fig. 13: Experimental and modeling bubble radius versus mixing time. Symbols "■♦" Refer to experimental and modeling results, respectively.

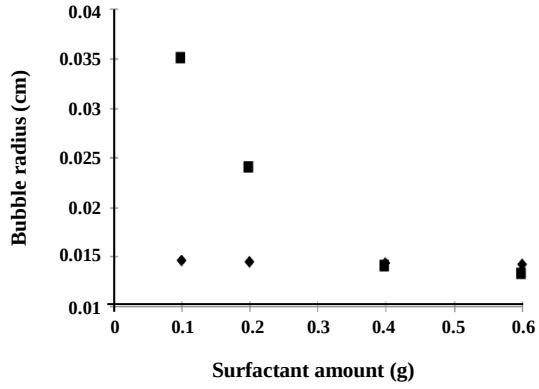

Fig. 14: Experimental and modeling bubble radius versus surfactant amount. Symbols "■♦" Refer to experimental and modeling results, respectively.

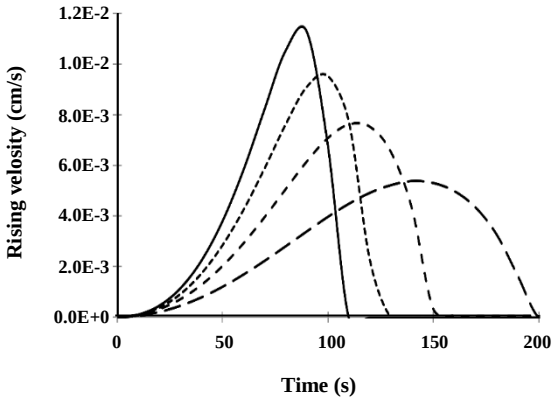

Fig. 15: Impact of blowing agent loading on single bubble rising velocity. Continuous, dot, dash, and long dash lines refer to 2, 1.5, 1, and 0.5 g loading of water.

which is much thicker than the critical thickness of $281\dot{A}$. This indicates the critical thickness is too thin to be generally reached within the bubble radius range in this study. Experimental film thickness was measured based on Figures 10 and 11. The actual film thickness was about $50000\,\dot{A}$, which means the simulation calculation was accurate. Therefore, this mode of failure was proved not happening in rigid foams.

Another possible reason causing foam failure may be due to bubbles rising during the foaming process. Bubbles close to the top surface may escape from the resin phase due to buoyancy and bubbles far from the top may coalesce with each other because a larger bubble has a faster-rising velocity than a small bubble which leads them to meet and coalesce. Moreover, if a bubble rises at a critical velocity, it may rupture due to shear force. The detailed impact of bubble rising on foam failure will be studied further. Fig. 15 presents a single bubble rising velocity versus time during the foaming process, and the impact of blowing agent loading was evaluated. Table 3 summarizes the modes of foam failure and the current status of these studies.

CONCLUSIONS

An initial critical analysis of how surfactants impact urethane foam-forming processes has been performed, which included a survey of the literature, a summary of available theory/models, and preliminary simulations. The following conclusions are a result of this analysis.

- Surfactants reduce the surface tension of bubble-resin interfaces resulting in the stabilization of higher concentrations of bubbles and bubble nucleation sites in resin mixtures.
- The combination of adequate mixing (associated energy input) and surfactants is necessary to form sufficient bubble nucleation sites at the onset of the urethane-foam-forming process to form the desired fine cell structures in quality urethane foams. Up to the limit of "adequate" mixing and surfactant loadings, longer mixing time and higher surfactant loading lead to more bubble counts and smaller bubble radius.
- Within the appropriate range of surfactant loadings, surface tension is a linear function of $\ln(C_{surf})$. Therefore the surface tension can be calculated based on the concentration of surfactant in solutions.
- Surfactants have minimal impact on reaction kinetics and thermodynamics for systems where the solubility of the reagents is not an issue.

Table 2: Modes of foam failure and current status of studies.

Related to Cell Size (Category 1)	
Course cell structure leading to poor thermal conductivity and low compression strength.	More/better surfactant increases the number of cell nucleation sites resulting in smaller gas cells in the foam
Related to Rate Of Rising Of Bubbles In Resin (Category 2)	
Bubbles rise in resin "liquid" and eventually escape through rupture of the top surface of the foam.	More/better surfactant leads to smaller gas bubbles that rise slower than large gas bubbles Simulation can be used to better understand how viscosity and bubble size translate to changing rise velocities of bubbles during foaming. Is there a critical bubble buoyancy-driven rise velocity that leads to failure?
The resin cures too slowly, resulting in low viscosity that allows bubbles to rise and escape.	
Rise of bubbles leads to concentration of bubbles at the top of resin where coalescing occurs in addition to surface rupture and escape.	
Rupture of Cells Dispersed In Matrix (Category 3)	
Bubble growth causing film thinning	Not applied. Critical thickness is too thin to be generally reached
*Bubble coalescing due to different rising velocity	Questionable. Bubble sizes and locations need to be specified and discussed
*Bubble rupture due to shear force	Questionable. Critical bubble rising velocity needs to be identified
Cascade collapse of rigid foam OR the desired "blow" of a flexible foam.	Complex phenomena. Could be due to pressure buildup in cells, herniating of cells at the surface of foam, and cascade herniating-type failures as pressures in upper cells reduce
Related to Final Resin Morphology	
Resin does not adequately cure to form a strong solid/elastic phase.	Not substantially related to surfactant.

- The MATLAB simulation successfully predicts bubble radius, inner pressure, and film thickness during the foaming process in addition to temperature and foam height profiles as long as surfactant is sufficient.
- The critical film thickness (as predicted by Redoev's model[31]) is too thin to be generally reached within the bubble radius range in this study.

The mechanisms through which surfactants lead to foam failure are not well-validated in the literature suggesting that the mechanisms are not well understood beyond the basic concept that surfactants can slow down the coalescing and rupturing of bubbles/cells in a foam. The key to better understanding the mechanisms through which surfactants lead to successful foam formation likely lies in the analysis of modes of foam failure and how surfactants reduce the modes of failure.

A conclusion of this analysis is that the impact of surfactants in foam formulations can be grouped into three categories, with each having different methods to critically investigate and understand as follows:

Category 1 – Role of surfactants in forming cell nucleation sites where the role of the surfactant is critically coupled with the energy input during mixing to form nucleation sites.

Category 2 – The surfactant plays a role in impacting nucleation sites. However, after that point, the inter-relationship of cell growth, viscosity, and buoyancy lead to velocity for bubble rise in the system. A rise velocity beyond a critical value could lead to failure.

Category 3 – As pressure builds in foam that is not fully set, weak spots of cells at the top of the foam could urinate leading to either a cascade collapse or the desire "blow" of flexible foam.

Both Category 2 and Category 3 types of failures involve the complex inter-relationship of how the cell grows during foaming, how pressure in the cell increases during foaming, and how viscosity increases. For these types of failures, no simply theory or model will adequately quantify the failure; simulation is needed.

Acknowledgments

The authors would like to thank Mustansiriyah University (www.uomustansiriyah.edu.iq) Baghdad-Iraq for its support in the present work.

Received : March 12, 2020 ; Accepted : Jul. 62020

REFERENCES

[1] Al-Moameri H.H., Hassan G., Jaber B., Simulation Physical and Chemical Blowing Agents for Polyurethane Foam Production. *IOP Conference Series: Materials Science and Engineering*. **518**: 062001 (2019).

[2] Al-Moameri H., Jaf L., Suppes G.J., Viscosity-Dependent Frequency Factor for Modeling Polymerization Kinetics, *RSC Advances*. **7(43)**: 26583-26592 (2017).

[3] Al-Moameri H.H., Jaf L.A., Suppes G.J., Simulation Approach to Learning Polymer Science. *J. Chem. Educ.* **95(9)**: 1554-1561 (2018).

[4] Al-Moameri H.H., Nabhan B.J., Wasmi M. T., Abdulrehman M.A., Impact of Blowing Agent-Blends on Polyurethane Foams Thermal and Mechanical Properties, *AIP Conference Proceedings*. **2213(1)**: 020177 (2020).

[5] Ganjeh-Anzabi P., Hadadi-Asl V., Salami-Kaljahi M., Roghani-Mamaqani H., A New Approach for Monte Carlo Simulation of RAFT Polymerization, *Iran. J. Chem. Chem. Eng. (IJCCE)*, **31(3)**: 75-84 (2012).

[6] Baser S.A., Khakhar D.V., Modeling of the Dynamics of Water and R-11 Blown Polyurethane Foam Formation, *Polymer Engineering and Science*, **34(8)**: 642 (1994).

[7] Baser S.A., Khakhar D.V., Modeling of the Dynamics of R-11 Blown Polyurethane Foam Formation. *Polymer Engineering and Science*. **34(8)**: 632-641 (1994).

[8] Harikrishnan G., Khakhar D.V., Modeling the Dynamics of Reactive Foaming and Film Thinning in Polyurethane Foams, *AIChE Journal*. **56(2)**: 522-530 (2010).

[9] Tesser R., Di Serio M., Sclafani A., Santacesaria E., Modeling of Polyurethane Foam Formation, *J. Appl. Polym. Sci.*, **92(3)**: 1875-1886 (2004).

[10] Mahmoudian M., Nosratzadegan K., Azarnia J., Esfadeh A., Ghasemi Kochameshki M., Shokri A., Modeling of Living Cationic Ring-Opening Polymerization of Cyclic Ethers: Active Chain End versus Activated Monomer Mechanism. *Iran. J. Chem. Chem. Eng. (IJCCE)*, **39(5)**: 95- 110 (2020).

[11] Zhang X.D., Macosko C.W., Davis H.T., Nikolov A.D., Wasan D.T., Role of Silicone Surfactant in Flexible Polyurethane Foam, *J. Colloid Interface Sci.*, **215(2)**: 270-279 (1999).

[12] Al-Moameri H., Ghoreishi R., Suppes G., Impact of Inter- and Intra-Molecular Movements on Thermoset Polymerization Reactions, *Chemical Engineering Science*. **161**: 14-23 (2017).

[13] Al-Moameri H., Ghoreishi R., Zhao Y., Suppes G.J., Impact of the Maximum Foam Reaction Temperature on Reducing Foam Shrinkage, *RSC Adv.* **5(22)**: 17171-17178 (2015).

[14] DOW, Dow Polyurethanes Flexible Foams.

[15] Al-Moameri H., Zhao Y., Ghoreishi R., Suppes G.J., Simulation of Liquid Physical Blowing Agents for Forming Rigid Urethane Foams, *J. Appl. Polym. Sci.* **132(34)**: 7- (2015).

[16] Al-Moameri H., Zhao Y., Ghoreishi R., Suppes G.J., Simulation Blowing Agent Performance, Cell Morphology, and Cell Pressure in Rigid Polyurethane Foams. *Ind Eng Chem Res*. **55(8)**: 2336-2344 (2016).

[17] Ghafoor Mohseni P., Shahrokhi M., Abedini H., Simulation, Optimization & Control of Styrene Bulk Polymerization in a Tubular Reactor, *Iran. J. Chem. Chem. Eng.(IJCCE)*, **32(4)**: 69-79 (2013).

[18] Hill, R.M., Silicone Surfactants - New Developments, *Curr. Opin. Colloid Interface Sci.* **7(5-6)**: 255-261 (2002).

[19] Yasunaga K., Neff R.A., Zhang X.D., Macosko C.W., Study of Cell Opening in Flexible Polyurethane Foam. *J. Cell Plast*. **32(5)**: 427-447 (1996).

[20] Kanner B., Decker T.G., Urethane Foam Formation - Role of the Silicone Surfactant. *J. Cell Plast.*, **5(1)**: 32-39 (1969).

[21] Al-Moameri H., Low Shrinkage Sustainable Bio-Based Polyol for Rigid Polyurethane Foam Production, *J. of Eng. and Sust. Dev.*, **22(2)**: - (2018).

[22] Burlatsky S.F., Atrazhev V.V., Dmitriev D.V., Sultanov V.I., Timokhina E.N., Ugolkova E.A., Tulyani S., Vincitore A., Surface Tension Model For Surfactant Solutions at the Critical Micelle Concentration, *J. Colloid Interface Sci.*, **393(1)**: 151-160 (2013).

[23] Abusaidi H., Ghaieni H.R., Ghorbani M., Influences of NCO/OH and triol/diol Ratios on the Mechanical Properties of Nitro-HTPB Based Polyurethane Elastomers, *Iran. J. Chem. Chem. Eng. (IJCCE)*, **36(5)**: 55-63 (2017).

[24] Hill R.M., Silicone Surfactants, *Taylor & Francis* (1999).
[25] Favelukis M., Albalak R.J., Bubble Growth in Viscous Newtonian and Non-Newtonian Liquids, *Chem. Eng. J.* **63(3)**: 149-155 (1996).
[26] Zhao Y., Gordon M.J., Tekeei A., Hsieh F.H., Suppes G.J., Modeling Reaction Kinetics of Rigid Polyurethane Foaming Process, *J. Appl. Polym. Sci.* **130(2)**: 1131-1138 (2013).
[27] Ghoreishi R., Zhao Y., Suppes G.J., Reaction Modeling of Urethane Polyols Using Fraction Primary Secondary and Hindered-Secondary Hydroxyl Content, *J. Appl. Polym. Sci.* **131(12)**: - (2014).
[28] Zhao Y., Zhong F., Tekeei A., Suppes G.J., Modeling Impact of Catalyst Loading on Polyurethane Foam Polymerization, *Applied Catalysis A: General*., **469**: 229-238 (2014).
[29] Nguyen A.V., Historical Note on the Stefan-Reynolds Equations, *J. Colloid Interface Sci.*, **231(1)**: 195- (2000).
[30] Ruckenstein E., Sharma A., A New Mechanism of Film Thinning: Enhancement of Reynolds' Velocity By Surface Waves. *J. Colloid Interface Sci.* **119(1)**: 1-13 (1987).
[31] Radoev B.P., Scheludko A.D., Manev E.D., Critical Thickness of Thin Liquid Films: Theory and Experiment, *J. Colloid Interface Sci.* **95(1)**: 254-265 (1983).
[32] Talaia M.A.R., Terminal Velocity of a Bubble Rise in a Liquid Column, *World Academy of Science, Engineering and Technology*, **28**: 264-268 (2007).